Novel DNA biosensor based on the out-of-equilibrium body potential method in silicon-on-insulator

Licinius Benea, Melania Popescu, Maryline Bawedin, Monica Simion, Irina Ionica

***Abstract*— In this paper, we applied the out-of-equilibrium body potential measurements in a silicon-on-insulator (SOI) structure as a mean of DNA detection. The biochips were manufactured by 3-glycidoxypropyltrimethoxysilane (GOPTMS) functionalization, and single stranded DNA probes corresponding to human papillomavirus (HPV) were grafted onto the surface.**

The physicochemical characteristics were assessed by contact angle, Fourier Transform Infrared Spectrometry (FTIR) and microarray technique. The effects of the bio-chemical attachments to the surface of SOI were evaluated by body potential measurements implemented in the Ψ-MOSFET configuration, typically used for electrical characterization of substrates.

Body potential measurements versus the back gate voltage were able to distinguish the shift induced by DNA molecules only and the signatures were related to target DNA concentrations. The proposed reading method is remarkable owing to the fact that (1) it measures a potential (in the order of 1V) instead of a low current, (2) it allows fast sweeping measurements and (3) it requires a gate voltage close to 0V which induces less stress on the molecules attached to the surface.

***Index Terms*— body potential, GOPTMS, HPV-DNA, microarray, out-of-equilibrium, Silicon-on-insulator, Ψ-MOSFET,**

This work was supported by the AGIR-POLE CLEPS project funded by the University of Grenoble Alpes, Campus France PHC Brancusi (project 38 395QA), by the European projects WayToGoFast and REMINDER and by the Romanian Ministry of Research and Innovation through PHC Brancusi Bilateral project – BIS-SOI (contract no. PNIII P3-3.1-PM-EN-FR-2016) and through the contract MiMoSa no. 36/2017. (Licinius Benea and Melania Popescu contributed equally to this work. Corresponding Authors: Irina Ionica, Melania Popescu and Monica Simion).

Licinius Benea is with IMEP-LaHC laboratory (CNRS UMR 5130), University Grenoble Alpes, Grenoble, France (licinius.benea@gmail.com).

Melania Popescu is with the National Institute for Research and Development in Microtechnologies, Bucharest, Romania (melania.banu@imt.ro).

Maryline Bawedin is with IMEP-LaHC laboratory (CNRS UMR 5130), University Grenoble Alpes, Grenoble, France (maryline.bawedin@grenoble-inp.fr).

Monica Simion is with the National Institute for Research and Development in Microtechnologies, Bucharest, Romania (moni304ro@gmail.com)

Irina Ionica is with IMEP-LaHC laboratory (CNRS UMR 5130), University Grenoble Alpes, Grenoble, France (irina.ionica@grenoble-inp.fr).

I. Introduction

DNA biosensors and microarrays rely on the attachment of single-stranded DNA (ssDNA) probe sequences onto a chemically-modified surface to recognize its complementary DNA target sequences by hybridization [1-3]. The DNA hybridization can be measured with optical or electrical transducers, linked to a readout element which converts the signal into information which can be processed by the user [4-6].

Optical biosensors are based mainly on fluorescent detection and label-free detection [7]. The optical microarray biosensing relies on fluorophores conjugated to the target molecules and employs optical microscopes or digital cameras as detectors [8,9]. This technique is used for early disease diagnosis, enabling the parallel detection of thousands of labelled gene fragments [10,11]. False-positive or false-negative hybridization signals may be ensued by DNA labelling, despite the impressive detection sensitivity, stability and easy handling of the fluorescent dyes [12,13]. Thus, special attention has been given to the detection methods which do not require fluorescent labelling [14].

Electrical biosensors provide label-free detection and are classified as amperometric/voltammetric, potentiometric, impedance and field-effect transistors (FET) [5,14]. Of all mentioned detection schemes, FET-based biosensors became popular due to their fast development as a result of nanoscaling [15], and advances have been brought by introducing nanomaterials and nanostructuring methods to these devices [16]. Thus, throughout nanoscaling the FET-devices traditionally developed on bulk or 3D semiconductor materials can be also based on 1D structures (i.e. carbon nanotubes - CNTs and silicon nanowires -SiNWs), and 2D structures (i.e. graphene, silicene, germanene, MoS_2) [16-19]. Si-based 1D structures have provided good sensitivity and selectivity in the detection of DNA, proteins and viruses thanks to the high surface-to-volume ratio of SiNWs [20,21]. The detection limits of DNA molecules were reported to be in the range of 100 pM - 1 fM [22,23]. However, NW-FETs have low output signals with high fluctuations generated by the reproducibility issues associated with their mass production [21,24,25]. In order to avoid those issues, silicon on insulator (SOI), measured by the Ψ-MOSFET (metal-oxide-semiconductor FET) method has been considered for its large

surface of detection [26]. In Ψ-MOSFET the channel appearing at the interface between the silicon film and the buried oxide (BOX) is controlled by the voltage applied on the bulk substrate used as a backgate (V_{BG}). Sensors based on the Ψ-MOSFET configuration have already proven their detection potential of (3-Aminopropyl)triethoxysilane (APTES) [27], gold nanoparticles [28], porphyrin [29] and molecules with electron-donating capabilities [30], or radiation sensors [31].

In this paper, the Ψ-MOSFET configuration was selected to demonstrate the proof-of-concept of out-of-equilibrium body potential for sensing for the following reasons: (1) out-of-equilibrium phenomena due to floating body effects are visible in SOI substrates and devices, (2) the large detection surface of the Ψ-MOSFET minimizes the stochastic effects and (3) the silicon film is thin enough to guarantee coupling between the channel at the buried oxide interface and the molecules deposited on the top of the SOI [26]. As in all the FET-like biosensors, the detection performance of DNA depends on the surface chemistry to provide hybridization efficiency and specificity [32], so this was our initial concern. The surface functionalization with 3-glycidoxypropyltrimethoxysilane (GOPTMS) allows the covalent attachment of single-stranded DNA probes (ssDNA) via an amino modification at 5' end of DNA [33-37]. Microarray technology was employed to assess the reproducibility of DNA immobilization and hybridization on the surface modified with GOPTMS, by employing probes and target sequences specific to the high-risk human papillomavirus type 16 (HPV 16) [38,39]. The body potential measurements were compared to the traditional electric current versus V_{BG} characteristics, in order to reveal the influence of the target DNA hybridization at different concentrations of DNA.

II. Experimental Section

A. Sample preparation

The experimental workflow is depicted in **Fig. 1**.

The first set of samples, prepared on simple Si substrates, was used solely to validate all processing steps as optimal and reproducible. Thus, after functionalizing the surface with GOPTMS, the process was verified by Fourier Transform Infrared Spectroscopy (FTIR) and contact angle measurements. The DNA probes' immobilization and hybridization with the target sequences were validated by fluorescent detection, using microarray technology and statistical analysis. The second set of samples was fabricated from silicon on insulator substrates and was employed for demonstrating the new electrical detection approach.

Functionalization with GOPTMS. The Si substrates (Siegert Wafer, Germany) used for microarray validation were cut into 2.5x2 cm^2 dices. The samples were cleaned from impurities and hydroxylated for 15 min in a freshly prepared Piranha solution (H_2SO_4:H_2O_2 3:1 v/v). The generated hydroxyl groups do not affect the thin gate oxide's topology and thickness and are essential for the uniform silanization of the surface [40,41]. The samples were finally rinsed with deionised water and dried under a nitrogen stream.

A functionalization method with GOPTMS (Sigma-Aldrich, Germany) under vapour-phase was applied in order to prevent the epoxy ring-opening, caused by reaction with water via nucleophilic addition [42]. It was performed in a sealed Petri dish [43], for 3 h 30 min, at 85 °C. There was no physical contact between the samples and the 2 mL of GOPTMS. At the end of the reaction, the dices were cleaned 6 times successively in absolute ethanol and deionised water and further dried under a nitrogen stream. The chemically modified silicon samples were cured for 30 min at 110 °C.

DNA preparation for biodetection. The oligonucleotide sequences (Biomers.net, Germany) employed in the electrical and fluorescent detection are presented in **Table S1** (please see ***Supporting Information***). The immobilization buffer and microarray spotting conditions were previously described in [44]. For electrical detection, we delivered 50 µM of the solution on each active area. The immobilization reaction was optimized by incubation overnight at 60 °C, in a humidity chamber. Afterwards, the samples were dried for 1 h at 110 °C and rinsed 3 times sequentially with (i) 2x SSC/0.1% w/v SDS (saline sodium citrate/sodium dodecyl sulphate); (ii) 1x SSC and (iii) DIW (deionized water) in order to remove the unbound probes.

For microarray experiments, the hybridization step was performed using Cy5-labelled target sequences with final concentrations of 1 µM, 0.1 µM and 0.01 µM, whereas for the electrical characterizations we employed the same concentrations of unlabelled sequences. The hybridization was carried out for 4 h [44] at 40 °C and the washing steps were realized as in [45].

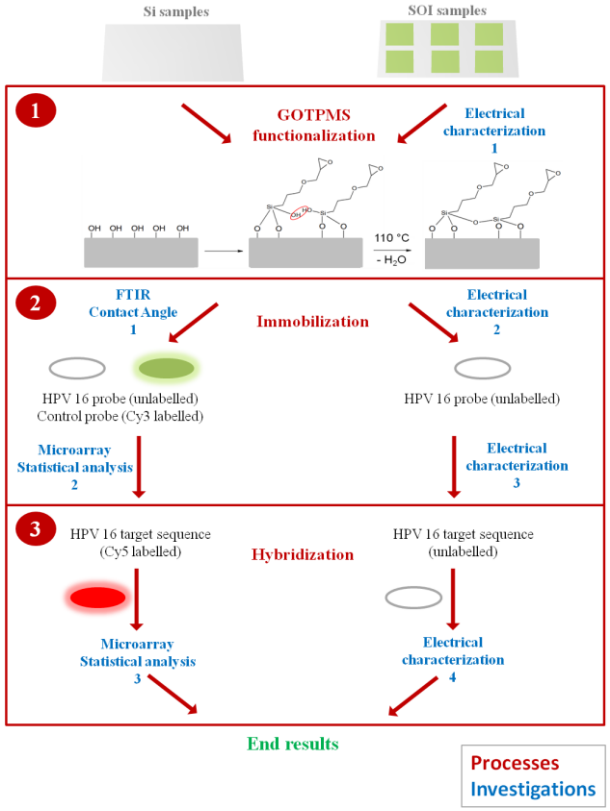

Fig. 1. Schematic representation of the experimental workflow

B. Functionalization and DNA grafting validation

The FTIR and the contact angle methods were employed to investigate the physicochemical properties of the GOPTMS-modified samples. The immobilization and hybridization efficiencies were assessed by microarray technology, given that it enables the parallel analysis of large sets of replicates.

Assessment of GOPTMS functionalization efficiency. A VERTEX 80/80v with RAM II FT-Raman Module (Bruker Optics, USA) was employed to study the surface functionalization with GOPTMS by FTIR spectrometry. The spectra were collected in a wavenumber interval of 5000-500 cm^{-1} and the analysis was performed using OPUS 7.5 Spectroscopy Software (Bruker Optics, USA).

Fig. 2 shows a typical attenuated total reflectance-FTIR (ATR-FTIR) spectra for Si functionalized with GOPTMS.

An expanded view of the region from 650 to 1500 cm^{-1} (**Fig. 2 (b)**) illustrates the peaks at 673 cm^{-1}, 708 cm^{-1}, 735 cm^{-1}, and 764 cm^{-1}, which are characteristic to the CH_2 rocking vibration mode in the Si-CH_2-R group. The bands at 796 cm^{-1}, 883 cm^{-1}, 906 cm^{-1}, 937 cm^{-1} and 1102 cm^{-1} can be assigned to the epoxide ring vibration modes. 1039 cm^{-1} is assigned to the Si-O-Si vibration [46,47], an indicator of the functionalization efficiency on Si, 1167 cm^{-1} is ascribed to the C-O stretching vibration and 1450 cm^{-1} corresponds to the asymmetrical deformation vibration of CH_3 [46]. A close-up view of the region from 2700 - 3100 cm^{-1} (**Fig. 2 (c)**) discloses peaks at 2920 at 3038 cm^{-1} which are attributed to the scissoring deformation of CH_2 [48] and the C-H stretching vibration corresponding to cycloalkane. The ATR-FTIR results confirm that GOPTMS has been successfully grafted on the Si surface.

The surface wettability of the functionalized substrates was determined at room temperature by employing the KSV Theta Optical Tensiometer equipment (Biolin Scientific, USA). Deionized water was used in the sessile drop tests, and the droplet volume was controlled using an automatic dispensing system. The graphical representation was generated after averaging the data acquired from three measurements (**Fig. 3**). An obvious increase in contact angle is the indicator of proper surface modification, induced by the epoxy groups and the methyl chains. These results are in accordance with the study of Goddard and Erickson [49] and confirm the appropriate functionalization with GOPTMS.

Microarray investigation of the immobilization and hybridization efficiencies. Immobilized DNA was detected with a laser scanning confocal fluorescence system (GeneTAC UC4 Microarray Scanner, Genomic Solutions, USA), by scanning the slides with a Cy3 (532 nm) excitation laser at 5 µm/pixel. The hybridized spots were detected by scanning the slides with a Cy5 (635 nm) excitation laser at a resolution of 5 µm/pixel. The coarse images were imported into GenePix® Pro 7 Software for quantifying the intensity of the immobilization and hybridization signals. The RStudio 1.1.463 [50] environment for R 3.5.3 [51] was used for processing and analysing the datasets based on 384 spot replicates per control probe and 256 spot replicates per each concentration of hybridized sequence. The graphics were generated using ggplot2 R package [52]. For the hybridization results, we employed background-corrected values normalized by a $\log_{10}$ transformation for a more meaningful and easier data interpretation [53]. The values placed further than 2σ (standard deviation) away from the mean were treated as outliers and removed from the graphical and statistical analysis.

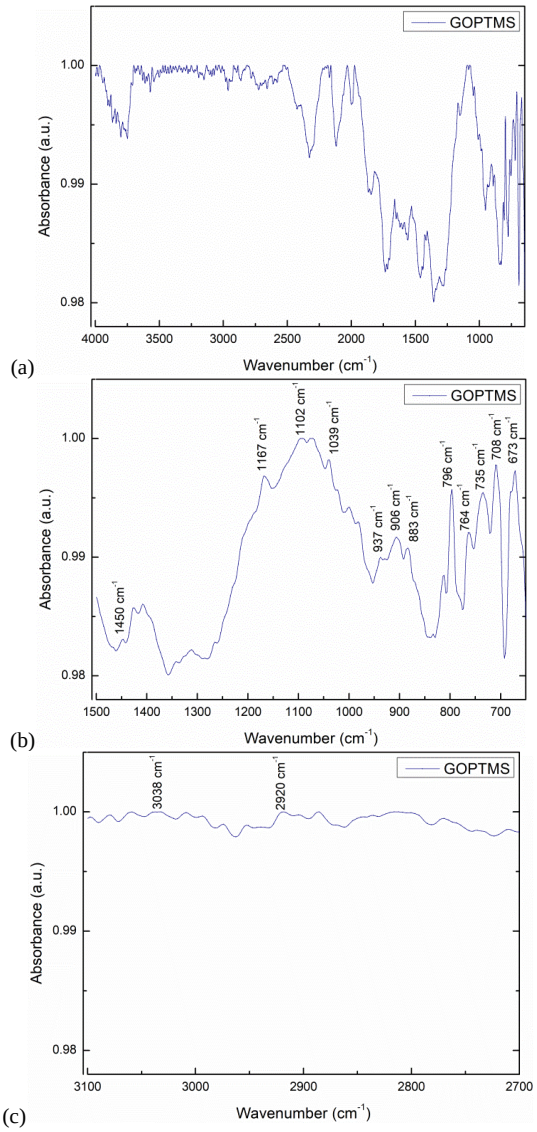

Fig. 2. ATR-FTIR of GOPTMS (a) full spectrum, (b) 650 - 1500 cm^{-1} region and (c) 2700 - 3100 cm^{-1} region

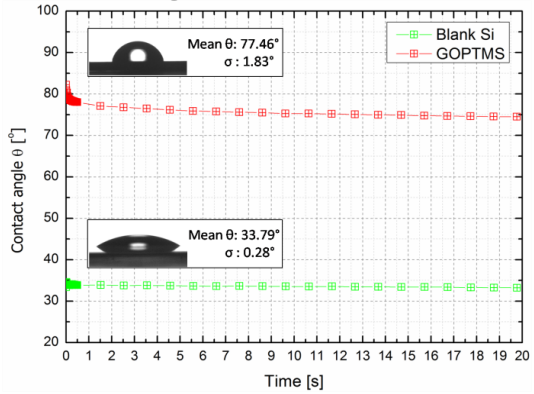

Fig. 3. Variation over time of the contact angle on blank silicon and on Si functionalized with GOPTMS

The measurement of the fluorescent signals corresponding to the immobilization step was done in order to confirm a proper probe attachment (**Fig. S1, *Supporting Information***). The stability of the chemical bond formed with the support was first tested by verifying the fluorescent signal after the immobilization and washing steps and second, after the hybridization and another washing round (**Fig. 4**).

According to the descriptive statistics, the loss in signal intensity, calculated for 384 replicate spots, was 13.39%, accompanied by a decrease of the standard deviation, which means that the unspecific tethered probes were discarded. The small difference between the average signal intensities is an indicator of a reliable, strong bond of the probes on GOPTMS-modified Si substrates.

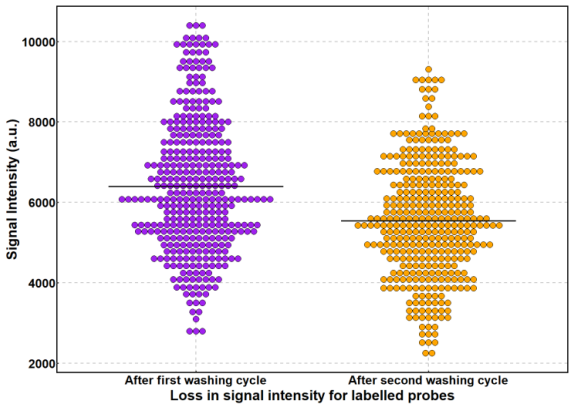

	Number of washing cycles	
	1st	2nd
Average	6399	5542
σ	1664.1	1429.8

Fig. 4. Fluorescent immobilization signals of the control sequences

For the SOI samples, the concentrations of 1 μM, 0.1 μM and 0.01 μM of target sequences specific to HPV 16 were used in hybridization (**Fig. S2, *Supporting Information***). The examination of the optical image is completed by the graphical analysis presented in **Fig. 5**, accompanied by their descriptive statistics. Per each target concentration, we employed 256 replicate spots in order to increase the statistical precision of the analysis [54].

Our observations, based on the fluorescent hybridization images, are confirmed by the graphical analysis, where the lowest signal intensity was recorded for 0.01 μM (3.19). For the 0.1 μM target sequences, we obtained an average signal intensity of 3.862 a.u. and a standard deviation of 0.342. As expected, the 1 μM hybridized target sequences exhibit an average signal intensity of 4.146 and a reduced data spreading ($\sigma = 0.155$).

The coefficient of variation (CV) of ≤10% is considered adequate [55], and it was calculated for assessing the reproducibility of the hybridization results using **Eq. 1**:

$$CV = \frac{\sigma}{\bar{I}} \times 100 \qquad (1)$$

where $\bar{I}$ is the average hybridization fluorescent intensity and σ is the standard deviation.

Taking into account the values obtained for all concentrations of target sequences, we obtained an improved CV value of 7.27 % which indicates the low variability of our microarray assay. Moreover, the good CV denotes indirectly the high reproducibility of the prior steps of microarray fabrication (surface functionalization and DNA immobilization).

After having proven the stability of the biochemical steps, we applied the procedure for the SOI samples that were to be used for the body potential method in the Ψ-MOSFET configuration for DNA detection.

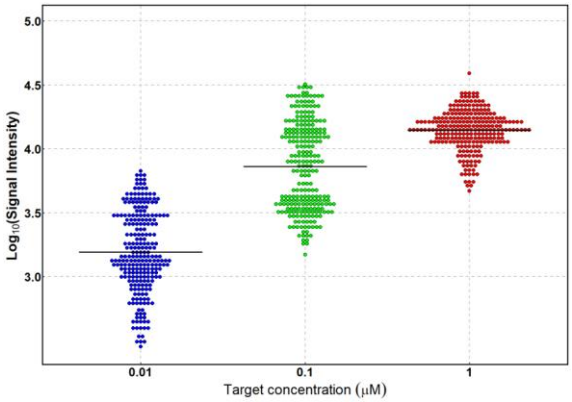

	DNA target concentration (μM)		
	0.01	**0.1**	**1**
Average	3.190	3.862	4.146
σ	0.318	0.342	0.155

Fig. 5. Graphical analysis of the fluorescent hybridization signals for three target DNA concentrations

C. Ψ-MOSFET method for SOI characterization

The proof of concept for the out-of-equilibrium body potential scanning will be realized using the Ψ-MOSFET configuration which is generally employed for SOI characterization [56]. The overview of the measuring structure, setup and electrical characteristics is depicted in **Fig. 6**.

For the Ψ-MOSFET measurements, islands of 5x5 mm² were patterned on the SOI wafers using photolithography and reactive ion etching (RIE) as illustrated in **Fig. 6(a)**. The innate upside-down structure of the SOI is highlighted: the bulk silicon substrate, acting as a gate, is biased using the chuck, while the BOX is used as a gate dielectric. In the conventional configuration, two probes are placed on the silicon film and act as the source and the drain of the pseudo-transistor as depicted in **Fig. 6(b)**. The electrical measurements were performed with an HP4155 Analyser and a 4-point probe Jandel station. The latter is provided with pressure controlled tungsten carbide probes positioned in line, at a distance of 1 mm from each other. The gate voltage (V_G) induces a channel at the interface between the top silicon film and the BOX. For low doping concentrations of the silicon film (i.e. 10^{15} cm^{-3}), the current between the source and the drain can be driven by either holes or electrons, depending on the polarity of V_G. Therefore, the drain current vs. gate voltage characteristics depicted in **Fig. 6(c)** present both an NMOS and a PMOS behaviour. There are two distinct V_G values that set the boundaries of the working regimes: the threshold voltage (V_T) marks the inversion and the flat-band voltage

(V_{FB}) marks the accumulation. They are extracted using the Y function method in order to avoid contact resistance [57]. Both those parameters will be employed to measure the response of the pseudo-transistor to the top surface functionalization.

The detection capabilities of the Ψ-MOSFET were previously evaluated from the I_D-V_G characteristics, based on V_T and V_{FB} extraction [28,58]. The measurements were realized in the linear regime (low V_D) and needed the use of a high gate voltage to set the inversion channel (V_G higher than the V_T). Note that a current shift measurement under the threshold regime could also be used for sensing, but the current levels are quite low. These principles are valid for other ISFET devices used as sensors, such as nanowires [22,25].

Herein, we employed the **out-of-equilibrium body potential** measurements in Ψ-MOSFET for sensing the charges deposited on the surface of the SOI film.

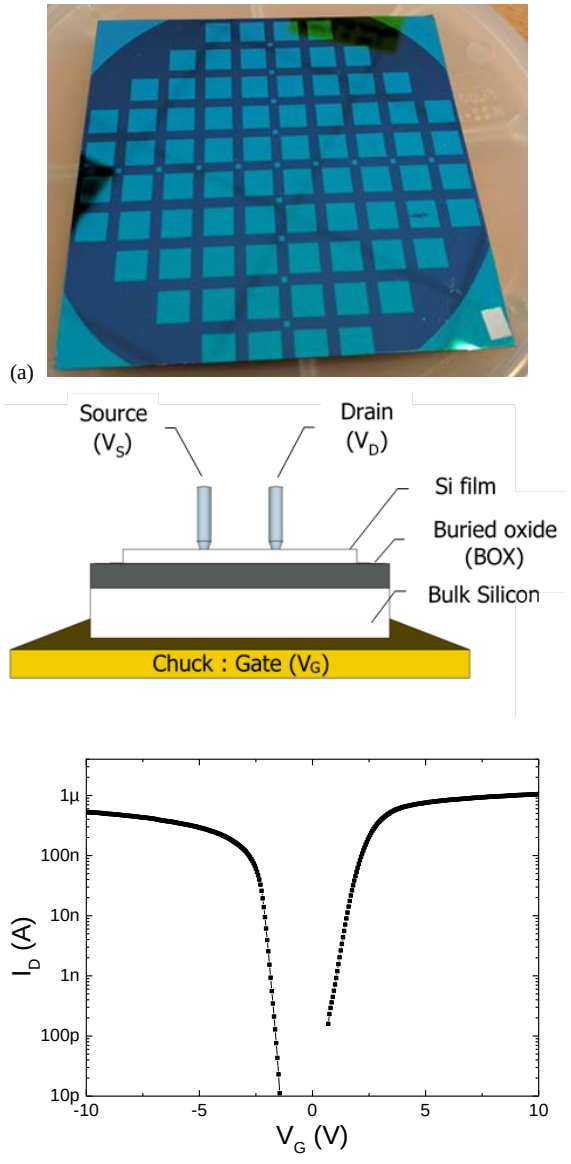

Fig. 6. Ψ-MOSFET (a) measuring structure; (b) experimental measurement setup; (c) drain current vs. gate voltage characteristics. V_D = 0.1 V, step 100 mV

III. Results and Discussion

A. Out-of-equilibrium body-potential measurements in the Ψ-MOSFET configuration

The experimental setup was modified by adding a third probe between the source and the drain in order to measure the body potential (V_B). The V_B measurement was realized using a zero current condition applied on the SMU (source-measurement unit) which has an input impedance of at least 10^{13} Ω.

Fig. 7 presents the drain current (I_D) and the body potential (V_B) curves obtained for different gate voltages. When the gate is swept from accumulation to inversion, the body potential increases with a quasi-linear behaviour, following V_G, and then sharply decreases when the inversion channel forms. The out-of-equilibrium body potential is large in the depletion region, where the drain current is negligible.

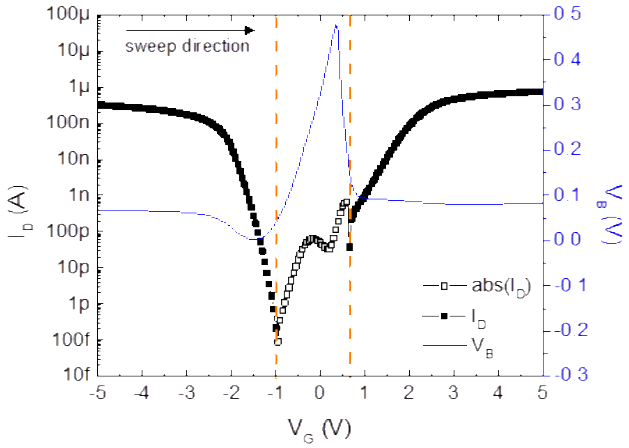

Fig. 7. Drain current and body potential vs. gate voltage sweep from accumulation to inversion. All the curves were measured simultaneously. V_D = 0.1 V, step 100 mV

The advantages of the body-potential compared to the classical drain current measurements in the Ψ-MOSFET configuration were already presented in a previous work [59]. It was shown that contrary to the current measurements in these structures [60], the out-of-equilibrium potential is independent of the position and the pressure applied on the probes. This constitutes a major advantage in terms of versatility for the sensor. However, the out-of-equilibrium body-potential is time-dependent [59], higher sweeping speeds showing higher V_B. This is advantageous since one can amplify the V_B response by realizing faster measurements. Nevertheless, choosing a measurement point that is relevant to a sensor application can be difficult. In order to determine a stable point that can be used to measure the shift in the body potential, various sweeping speeds were employed **(Fig. 8)**.

The various sweeping speeds were obtained by modifying the delay time (time between two consecutive measurement points), the integration time (time to obtain one measurement point) and the V_G step. Obviously, the only stable point is the one which marks the beginning of the out-of-equilibrium regime. This point, noted V_{B0}, will be used in the next section for sensing applications.

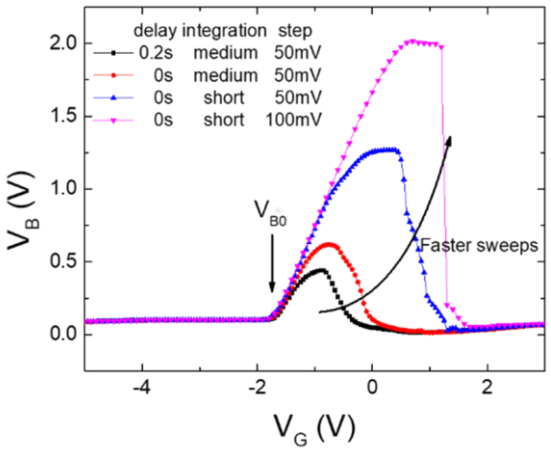

Fig. 8. Body potential vs. gate voltage characteristics for different sweeping speeds obtained by varying the delay time, the integration time and the size of the measurement step.

B. Electrical detection of DNA using the out-of-equilibrium body potential

The measurements of the I_D-V_G and V_B-V_G curves were performed after every functionalization step. The graphical representation in **Fig. 9** is an example of the obtained characteristics after each experimental step for one of the devices. The presence of GOPTMS induced a positive shift, whereas the immobilization and hybridization steps induced a negative shift in both I_D-V_G and V_B-V_G curves. This behaviour is representative for the ensemble of the measured devices.

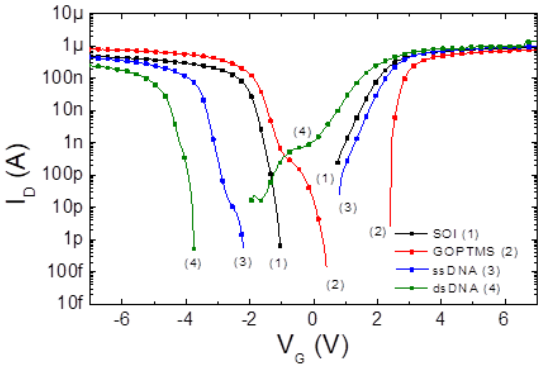

(a)

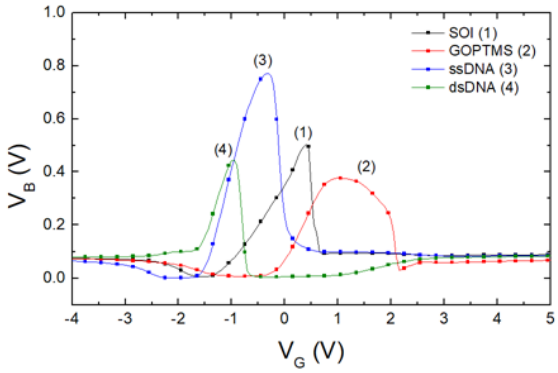

(b)

Fig. 9. Drain current vs. gate voltage (a) and body potential vs. gate voltage (b) for various stages of biochip processing. t_{Si} = 88nm and t_{BOX} = 145nm.

For the experimental reproducibility, 16 devices were fabricated from an SOI wafer with an 88 nm thick silicon film and a 145 nm thick BOX. They were all submitted to GOPTMS and probe DNA attachment. For the hybridization step, they were distributed into 4 groups according to the concentrations of the target DNA contained in the hybridization buffer: 0 µM (bare buffer solution), 0.01 µM, 0.1 µM and 1 µM, respectively.

In order to have a global view of the shifts induced by every step on each structure, the relative variation of the threshold voltage (ΔV_T) and the flat-band (ΔV_{FB}) voltage were presented as box plots (**Fig. 10**).

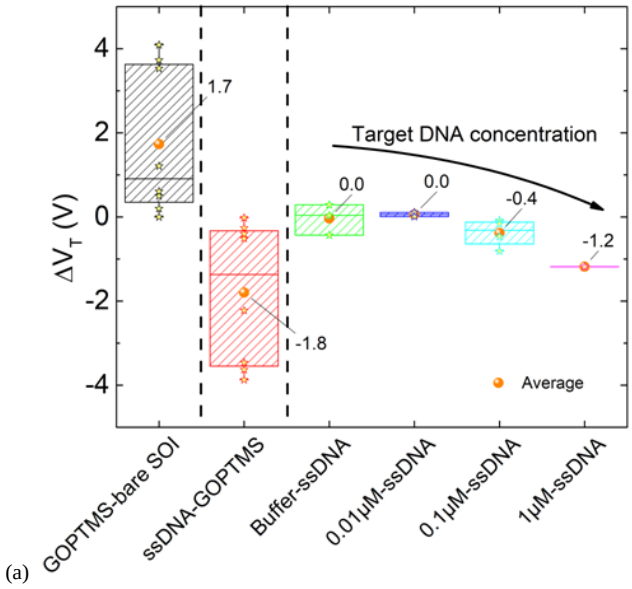

(a)

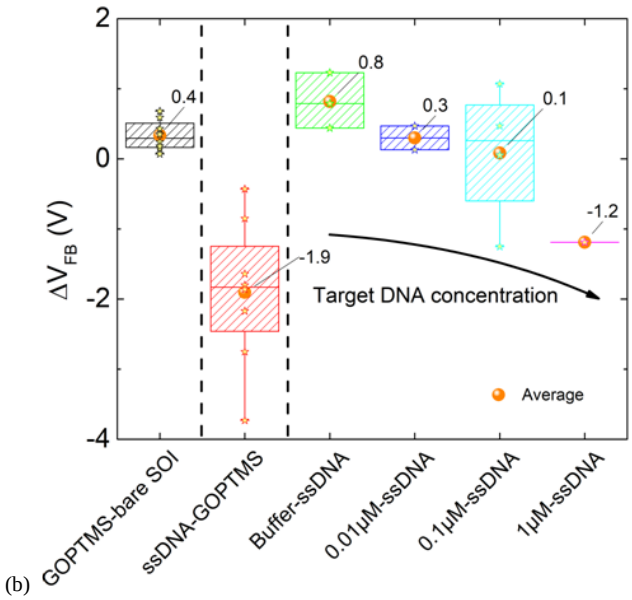

(b)

Fig. 10. Relative variations of (a) V_T and (b) V_{FB} for various stages of biochip processing. Parameter extraction results for the thick film/ BOX measurements. t_{Si} = 88nm and t_{BOX} = 145nm.

The relative variations were calculated as the difference in threshold or flat-band voltage after and before every functionalization step. The presence of GOPTMS induced a positive ΔV_T and ΔV_{FB} due to the negative charges added on the top surface, which resulted from the intermolecular interactions through the silane crosslinking [61]. The ssDNA immobilization induced a negative average shift of -1.8 V for the threshold voltage, and -1.9 V for the flat-band voltage, in opposition to the negative charge of the DNA. The addition of the buffer solution induces a negligible shift on the threshold voltage and a small positive shift on the flat-band voltage. A negative shift is obtained by introducing concentrations of 0.01 µM, 0.1 µM and 1 µM of target DNA into the buffer solution, lowering the values of ΔV_T and ΔV_{FB} with the increase of the DNA concentration. This behaviour was also observed in other FET-based sensors [62,63], and it was attributed to the charge inversion of the DNA molecule. This is a counterintuitive phenomenon in which the DNA molecule – a polyanion – attracts opposite charges in excess of its own nominal charge, so that its charge changes its sign [64-66]. Positive charges can come from the immobilization and hybridization solutions employed, which were rich in Na^+ ions that might have shielded the overall negative charge of DNA molecules. It is possible that, after the washing steps, the Na^+ ions remained attached mostly to the O1P atoms in the pentose phosphate backbone of the DNA strains [67].

However, it is worth noting again that even if the sign is counterintuitive with respect to the actual charge of the DNA, both V_T and V_{FB} variations are following the DNA concentration in the samples.

The shifts in V_B – V_G are consistent with the current measurements as illustrated in **Fig. 9b**. For a more quantitative analysis, the V_G position of the V_{B0} point ($V_G@V_{B0}$) was extracted from the raw data of all the samples and the relative variations between 2 consecutive steps were calculated for ΔV_T and ΔV_{FB}. The relative variations measured in V_G at V_{B0} position (ΔV_G @V_{B0}) are displayed in **Fig. 11** for a forward sweeping direction (gate voltage from negative to positive).

Indeed, ΔV_G @V_{B0} follows the same trends as ΔV_T and ΔV_{FB}. The V_{B0} shift induced by GOPTMS is positive, while for DNA immobilization it is negative. For hybridization, the measurements show a clear negative trend, which increases with DNA concentration, proving that these types of measurements are exclusively sensitive to the DNA molecule and not the result of the buffer solution.

The results show that the body-potential method is able to perfectly match the results obtained from the conventional current measurements in the Ψ-MOSFET configuration. The main advantage of this method is that it can exploit the subthreshold regime of a device while measuring a potential instead of a very low current. With a careful choice of device characteristics, the measuring can be realized at gate voltages close to 0 V, which is very advantageous because (1) the molecular layer is less disturbed by the electric field and (2) it emphasizes the charge effect of the molecule as opposed to its dielectric effect as described in [68].

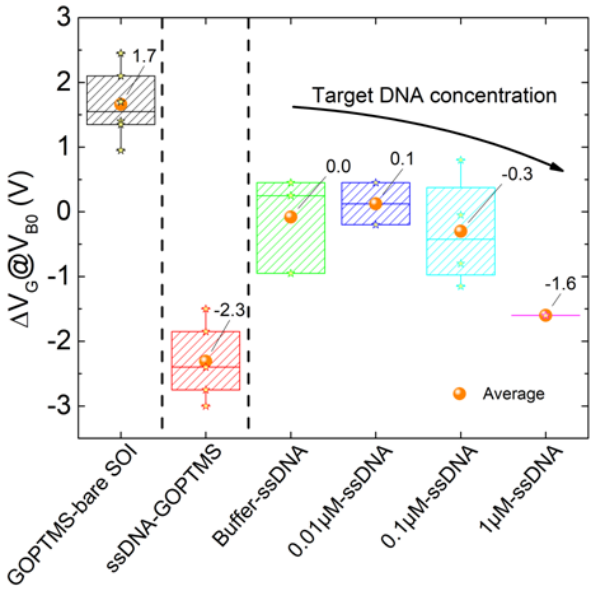

Fig. 11. Relative variations of the V_G corresponding to V_{B0} point for different stages of biochip functionalization. t_{Si} = 88nm and t_{BOX} = 145nm.

Limit of detection of the body potential method. All results considered, one can estimate the limit of detection of the Ψ-MOSFET structure at 1µM of target DNA (for ΔV_T, ΔV_{FB}, and $\Delta V_G@V_{B0}$). This is very high compared to the nanowire counterparts, which can reach 1 fM [23,24,69-72]. This is mainly determined by the very large surface of our device. The shifts observed in field-effect structures are proportional to the density of charges added by the chemical species, thus the surface of the device should be considered. The equivalent limit of detection for a smaller device can be roughly approximated using the ratio of the active surfaces. In our case, a 4 mm in diameter drop of DNA solution (obtained by visual estimation) deposited on the SOI covers a surface of 50 mm², whereas a nanowire with a typical geometry of 10 µm in length and a height and width of 50 nm has a sensing area of $1.5 \cdot 10^{-6}$ mm² (considering the three exposed sides of the device). The difference of surface would lead to an equivalent limit of detection of 30 fM for our method if the active surface was the one of a nanowire. Consequently, the detection limit is in line with the one in nanowires.

The reduction of the surface of the device would be therefore necessary in order to improve the limit of detection. However, as evidenced in [73], the size of the device needs to be carefully chosen, since the extreme miniaturization can have detrimental effects on the magnitude of the body potential.

IV. Conclusions

Our study proposes a novel detection paradigm for field-effect biosensors based on the measurement of the out-of-equilibrium body potential in thin film silicon-on-insulator, instead of the classical conduction/current. This method can be employed for detecting bacteria and viruses responsible for various disease states.

A functionalization strategy based on GOPTMS was developed. The chemical and physical properties of the GOPTMS-modified samples, examined by FTIR and contact

angle, have shown a successful modification of the surface. By microarray investigation, using a large number of spot replicates, we have shown low experimental variability, efficient probe DNA grafting and target recognition.

The out-of-equilibrium body potential was measured for thin film SOI samples in the Ψ-MOSFET configuration and correlated with the charge deposited on the surface by functionalization. The measurement of the body-potential, realized close to V_G = 0V, where the current in the device is negligible, can be advantageous for detection, since it could potentially simplify the measurement setup. An additional key element is that, unlike the I_D-V_G, V_B measurements proved to be invariable to the position and the pressure applied on the probes. For samples with various concentrations of DNA, the body-potential response is correlated with the concentration. Using this method, we were able to detect DNA hybridization with a limit of detection of 1 µM. However, this relatively high value is related to the high surface of our device and could be improved by a reduction in size. Based on this proof of concept, the out-of-equilibrium potential reading could be extended towards other field-effect structures.

ACKNOWLEDGMENT

The authors thank Cécile Delacour for inspiring comments and SOITEC for the samples.

REFERENCES

[1] M. Yang, M. E. Mcgovem, and M. Thompson, "Genosensor technology and the detection of interfacial nucleic acid chemistry", *Anal. Chim. Acta*, vol. 346, pp. 259–275, 1997.

[2] F. R. R. Teles and L. P. Fonseca, "Trends in DNA biosensors", *Talanta*, vol. 77, no. 2, pp. 606–623, 2008.

[3] A. Sassolas, B. D. Leca-Bouvier, and L. J. Blum, "DNA biosensors and microarrays", *Chem. Rev.*, vol. 108, no. 1, pp. 109–139, 2008.

[4] J. Wang, "From DNA biosensors to gene chips", *Nucleic Acids Res.*, vol. 28, pp. 3011-3016, 2000.

[5] M. Gabig-Ciminska, "Developing nucleic acid-based electrical detection systems", *Microb. Cell Fact.*, vol. 5, pp. 1–8, 2006.

[6] A. Munawar, Y. Ong, R. Schirhagl, M. A. Tahir, W. S. Khan, and S. Z. Bajwa, "Nanosensors for diagnosis with optical, electric and mechanical transducers", *RSC Adv.*, vol. 9, no. 12, pp. 6793–6803, 2019.

[7] X. Fan, I. M. White, S. I. Shopova, H. Zhu, J. D. Suter, and Y. Sun, "Sensitive optical biosensors for unlabeled targets : A review", *Anal. Chim. Acta*, vol. 620, pp. 8–26, 2008.

[8] J. A. B. Tech *et al.*, "Analytical & bioanalytical techniques optical and electrical Si-based biosensors : fabrication and trasduction issues", *J. Anal. Bioanal. Tech.*, no. 12, pp. 1-6, 2014.

[9] L. De Stefano *et al.*, "DNA optical detection based on porous silicon technology: From biosensors to biochips", *Sensors*, vol. 7, no. 2, pp. 214–221, 2007.

[10] J.S. Lee, J.J. Song, R. Deaton, J. Kim, Assessing the detection capacity of microarrays as bio / nanosensing platforms, BioMed Res. Int. 2013 (2013) 1-8. [1] J. S. Lee, J. J. Song, R. Deaton, and J. Kim, "Assessing the detection capacity of microarrays as bio / nanosensing platforms", *BioMed Res. Int.*, vol. 2013, pp. 1-8, 2013.

[11] S. L. Lai, C.-H. Chen, and K.-L. Yang, "Enhancing the fluorescence intensity of DNA microarrays by using cationic surfactants.", *Langmuir*, vol. 27, no. 9, pp. 5659–64, 2011.

[12] A. Malossini, E. Blanzieri, and R. T. Ng, "Detecting potential labeling errors in microarrays by data perturbation", *Bioinformatics*, vol. 22, no. 17, pp. 2114–2121, 2006.

[13] A. Syahir, K. Usui, K. Tomizaki, K. Kajikawa, and H. Mihara, "Label and label-free detection techniques for protein microarrays", *Microarrays*, vol. 4, no. 2, pp. 228–244, 2015.

[14] X. Luo and J. J. Davis, "Electrical biosensors and the label free detection of protein disease biomarkers", *Chem. Soc. Rev.*, vol. 42, no. 13, pp. 5944–5962, 2013.

[15] Y. C. Syu, W. E. Hsu, and C. T. Lin, "Review-field-effect transistor biosensing: Devices and clinical applications", *ECS J. Solid State Sci. Technol.*, vol. 7, no. 7, pp. Q3196–Q3207, 2018.

[16] J. L. Hammond, N. Formisano, P. Estrela, S. Carrara, and J. Tkac, "Electrochemical biosensors and nanobiosensors", *Essays Biochem.*, vol. 60, pp. 69–80, 2016.

[17] D. Di Felice and Y. J. Dappe, "2D vertical field-effect transistor", *Nanotechnology*, vol. 29, no. 50, pp. 1-11, 2018.

[18] Q. Qian *et al.*, "2D materials as semiconducting gate for field-effect transistors with inherent over-voltage protection and boosted ON-current", *Npj 2D Mater. Appl.*, vol. 3, no. 1, pp. 1-9, 2019.

[19] M. Chhowalla, D. Jena, and H. Zhang, "Two-dimensional semiconductors for transistors", *Nat. Rev. Mater.*, vol. 1, no. 11, pp. 1–15, 2016.

[20] M. Kaisti, "Detection principles of biological and chemical FET sensors," *Biosens. Bioelectron.*, vol. 98, pp. 437–448, 2017.

[21] F. Patolsky and C.M. Lieber, "Nanowire nanosensors", *Mater. Today.*, vol. 8, pp. 20-28, 2005.

[22] T. Adam and U. Hashim, "Highly sensitive silicon nanowire biosensor with novel Liquid gate control for detection of specific single-stranded DNA molecules", *Biosens. Bioelectron.*, vol. 67, pp. 656–661, 2015.

[23] G. Wenga, E. Jacques, A.C. Salaün, R. Rogel, L. Pichon and F. Geneste, "Step-gate P nanowires field effect transistor compatible with CMOS technology for label-free DNA biosensor", *Biosens. Bioelectron.*, vol. 40, pp. 141-146, 2013.

[24] J. Hahm and C.M. Lieber, "Direct ultrasensitive electrical detection of DNA and DNA sequence variations using nanowire nanosensors", *Nano Lett.*, vol.4, pp. 51-54, 2004.

[25] X. Gong, R. Zhao and X. Yu, "A 3-D-silicon nanowire FET biosensor based on a novel hybrid process", *J. Microeelectromechanical Syst.*, vol. 27, pp. 1–7, 2018.

[26] S. Cristoloveanu, D. Munteanu and M.S.T. Liu, "A review of the pseudo-MOS transistor in SOI wafers: Operation, parameter extraction, and applications", *IEEE Trans. Electron Devices.*, vol. 47, pp. 1018–1027, 2000.

[27] C. Fernandez, N. Rodriguez, C. Marquez and F. Gamiz, "Determination of ad hoc deposited charge on bare SOI wafers", Presented at EUROSOI-ULIS 2015: 2015 Joint International EUROSOI Workshop and International Conference on Ultimate Integration on Silicon. Available: https://ieeexplore.ieee.org/document/7063830

[28] I. Ionica, A.E.H. Diab and S. Cristoloveanu, Gold nanoparticles detection using intrinsic SOI-based sensor, 11th IEEE International Conference on Nanotechnology.
Available: https://ieeexplore.ieee.org/document/6144565

[29] F. Duclairoir, L. Dubois, A. Calborean, A. Fateeva, B. Fleury, A. Kalaiselvan, J.C. Marchon, P. Maldivi, M. Billon, G. Bidan and B. Salvo, "Bistable molecules development and Si surface grafting: two chemical tools used for the fabrication of hybrid molecule/Si CMOS component", *Int. J. Nanotechnol.*, vol. 7, pp. 719-737, 2010.

[30] T. He, J. He, M. Lu, B. Chen, H. Pang, W.F. Reus, W.M. Nolte, D.P. Nackashi, P.D. Franzon and J.M. Tour, "Controlled modulation of conductance in silicon devices by molecular monolayers", *J. Am. Chem. Soc.*, vol. 128, pp. 14537–14541, 2006.

[31] S.H. Jung, J.M. Kim, L.M. Jung, Y.H. Lee, S. Cristoloveanu, Y.H. Bae, "Pseudo-MOSFET analysis of proton irradiated and annealed SOI wafer", *ECS Trans.*, vol. 19, pp. 329–334, 2009.

[32] M.D. Sonawane and S.B. Nimse, "Surface modification chemistries of materials used in diagnostic platforms with biomolecules", *J. Chem.*, vol. 2016, pp. 1-19, 2016.

[33] F.F. Tao and S.L. Bernasek, "Functionalization of Semiconductor Surfaces", John Wiley & Sons, Hoboken, New Jersey, 2012.

[34] S. Russell, L. Meadows and R. Russell, "Chapter 3: Designing and Producing Microarray", in: Microarray Technology in Practice, Elsevier, 2008, pp. 36-70, ISBN: 978-0-12-372516-5.

[35] S. Nimse, K. Song, M. Sonawane, D. Sayyed and T. Kim, "Immobilization techniques for microarray: challenges and applications", *Sensors.*, vol. 14, pp. 22208–22229, 2014.

[36] A.K.Y. Wong and U.J. Krull, "Surface characterization of 3-glycidoxypropyltrimethoxysilane films on silicon-based substrates", *Anal. Bioanal. Chem.*, vol. 383, pp. 187–200, 2005.

[37] I. Luzinov, D. Julthongpiput, A. Liebmann-vinson, T. Cregger, M.D. Foster and V.V Tsukruk, "Epoxy-terminated self-assembled

monolayers : molecular glues for polymer layers", *Langmuir*, vol. 16, pp. 504–516, 2000.
[38] Y. Chen, V. Williams, M. Filippova, V. Filippov and P. Duerksen-Hughes, "Viral carcinogenesis: factors inducing DNA damage and virus integration", *Cancers*, vol 6, pp. 2155–2186, 2014.
[39] D. Hanahan and R.A. Weinberg, "The hallmarks of cancer", *Cell.*, vol. 100, pp. 57–70, 2000.
[40] S.D. Chandradoss, A.C. Haagsma, Y.K. Lee, J.H. Hwang, J.M. Nam and C. Joo, "Surface passivation for single-molecule protein studies", *J. Vis. Exp.*, vol. 86, pp. 4–11, 2014.
[41] Y. Han, D. Mayer, A. Offenhäusser and S. Ingebrandt, "Surface activation of thin silicon oxides by wet cleaning and silanization", *Thin Solid Films.*, vol. 510, pp. 175–180, 2006.
[42] S.J. Stropoli and M.J. Elrod, "Assessing the potential for the reactions of epoxides with amines on secondary organic aerosol particles", *J. Phys. Chem. A.*, vol. 119, pp. 10181–10189, 2015.
[43] S. Williams, P. Davies, J. Bowen and C. Allender, "Controlling the nanoscale patterning of AuNPs on silicon surfaces", *Nanomaterials.*, vol. 3, pp. 192–203, 2013.
[44] M. Banu, M. Simion, P. Varasteanu, L. Savu, and I. Farcasanu, "Microarray and Surface Plasmon Resonance experiments for HPV genotyping on Au-supports," vol. 20, no. 4, pp. 426–439, 2017.
[45] M. Banu, M. Simion, M.C. Popescu, P. Varasteanu, M. Kusko and I.C. Farcasanu, "Specific detection of stable single nucleobase mismatch using SU-8 coated silicon nanowires platform", *Talanta.*, vol. 185, pp. 281-290. 2018.
[46] D.K. Shukla, S.V. Kasisomayajula and V. Parameswaran, "Epoxy composites using functionalized alumina platelets as reinforcements", *Compos. Sci. Technol.*vol. 68, pp. 3055–3063, 2008.
[47] H. Yim, M.S. Kent, D.R. Tallant, M.J. Garcia amd J. Majewski, "Hygrothermal degradation of (3-glycidoxypropyl)trimethoxysilane films studied by neutron and X-ray reflectivity and attenuated total reflection infrared spectroscopy", *Langmuir.*, vol. 21, pp. 4382–4392, 2005.
[48] M. Mandhakini, T. Lakshmikandhan, A. Chandramohan and M. Alagar, "Effect of nanoalumina on the tribology performance of C4-ether-linked bismaleimide-toughened epoxy nanocomposites", *Tribol. Lett.*, vol. 54, pp. 67–79, 2014.
[49] J.M. Goddard and D. Erickson, "Bioconjugation techniques for microfluidic biosensors", *Anal. Bioanal. Chem.*, vol. 394, pp. 469–479, 2009.
[50] RStudio: Integrated development environment for R (Version 1.1.463) [Computer software]. Boston, MA. Retrieved January 2019.
[51] R Core Team, R: a Language and Environment for Statistical Computing, R Foundation for Statistical Computing, Vienna, Austria, 2016. Available: https://www.r-project.org/
[52] H. Wickham, ggplot2: Elegant Graphics for Data Analysis, Springer-Verlag, New York, 2009.
[53] S. Draghici, "Multiple Comparisons, in: Data Analysis Tools for DNA microarrays", Chapman and Hall/CRC Mathematical Biology and Medicine Series, Boca Raton, Florida, 2003.
[54] N. Malo, J.A. Hanley, S. Cerquozzi, J. Pelletier, R. Nadon, "Statistical practice in high-throughput screening data analysis", *Nat. Biotechnol.*, vol. 24, pp. 167–175, 2006.
[55] G.F. Reed, F. Lynn and B.D. Meade, "Quantitative Assays", *Clin. Diagn. Lab. Immunol.*, vol. 9, pp. 1235–1239, 2002.
[56] S. Williams, S. Cristoloveanu and G. Campisi, "Point contact pseudo-metal/oxide/semiconductor transistor in as-grown silicon on insulator wafers", *Mater. Sci. Eng. B.*, vol. 12, pp. 191–194, 1992.
[57] G. Ghibaudo, "New method for the extraction of MOSFET parameters", *Electron. Lett.*, vol. 24, pp. 543-545, 1988.
[58] L. Benea, M. Banu, M. Bawedin, C. Delacour, M. Simion, M. Kusko, S. Cristoloveanu and I. Ionica, "ψ-MOSFET configuration for DNA detection", Proc. Int. Semicond. Conf. CAS. Available: https://ieeexplore.ieee.org/document/8539753
[59] L. Benea, M. Bawedin, C. Delacour and I. Ionica, "Out-of-equilibrium body potential measurements in pseudo-MOSFET for sensing applications", *Solid-State Electron.*, vol. 143, pp. 69–76, 2018.
[60] L. Pirro, I. Ionica, G. Ghibaudo and S. Cristoloveanu, "Split-CV for pseudo-MOSFET characterization: Experimental setups and associated parameter extraction methods", 2014 International Conference on Microelectronic Test Structures (ICMTS). Available: https://ieeexplore.ieee.org/document/6841461
[61] Y. Paska and H. Haick, "Controlling surface energetics of silicon by intermolecular interactions between parallel self-assembled molecular dipoles", *J. Phys. Chem. C.*, vol. 113, pp. 1993–1997, 2009.
[62] T. Thu, T. Nguyen, M. Legallais, F. Morisot, T. Cazimajou and V. Stambouli, "First evidence of superiority of Si nanonet field effect transistors over multi-parallel Si nanowire ones in view of electrical DNA hybridization detection", *Mater. Res. Express*, vol. 6, pp. 1-9 2019.
[63] C.H. Kim, C. Jung, H.G. Park and Y.K. Choi, "Novel dielectric-modulated field-effect transistor for label-free DNA detection", *Biochip J.*, vol. 2, pp. 127–134, 2009.
[64] Y. Wang, R. Wang, B. Cao, Z. Guo and G. Yang, "Single molecular demonstration of modulating charge inversion of DNA", *Nat. Publ. Gr.*, pp. 1–11, 2016.
[65] B. Luan and A. Aksimentiev, "Electric and electrophoretic inversion of the DNA charge in multivalent electrolytes", *Soft Matter.*, vol. 6, pp. 243-246, 2010.
[66] A.A. Kornyshev, "Physics of DNA: unravelling hidden abilities encoded in the structure of 'the most important molecule'", *Phys. Chem. Chem. Phys.*, vol. 12, pp. 12352-12378, 2010.
[67] Y. Cheng, N. Korolev, and L. Nordenskio, "Similarities and differences in interaction of K + and Na + with condensed ordered DNA. A molecular dynamics computer simulation study", Nucl. Acid. Res., vol. 34, no. 2, pp. 686–696, 2006.
[68] J.H. Ahn, S.J. Choi, M. Im, S. Kim, C.H. Kim, J.Y. Kim, T.J. Park, S.Y. Lee and Y.K. Choi, "Charge and dielectric effects of biomolecules on electrical characteristics of nanowire FET biosensors", *Appl. Phys. Lett.*, vol. 111, pp. 113701-1 - 113701-5, 2017.
[69] E. Stern, A. Vacic and M.A. Reed, "Semiconducting nanowire Field-Effect Transistor biomolecular sensors", *IEEE Trans. Electron Devices.*, vol. 55, pp. 3119–3130, 2008.
[70] G.J. Zhang, J.H. Chua, R.E. Chee, A. Agarwal, S.M. Wong, K.D. Buddharaju and N. Balasubramanian, "Highly sensitive measurements of PNA-DNA hybridization using oxide-etched silicon nanowire biosensors", *Biosens. Bioelectron.*, vol. 23, pp. 1701–1707, 2008.
[71] C.J. Chu, C.S. Yeh, C.K. Liao, L.C. Tsai, C.M. Huang, H.Y. Lin, J.J. Shyue, Y.T. Chen and C.D. Chen, "Improving nanowire sensing capability by electrical field alignment of surface probing molecules", *Nano Lett.*, vol. 13, pp. 2564–2569, 2013.
[72] A. Gao, N. Zou, P. Dai, N. Lu, T. Li, Y. Wang, J. Zhao and H. Mao, "Signal-to-noise ratio enhancement of silicon nanowires biosensor with rolling circle amplification", *Nano Lett.*, vol. 13, pp. 4123–4130, 2013.
[73] M. Bawedin, S. Cristoloveanu, D. Flandre, and F. Udrea, 'Dynamic body potential variation in FD SOI MOSFETs operated in deep non-equilibrium regime: Model and applications', Solid-State Electron., vol. 54, no. 2, pp. 104–114, Feb. 2010, doi: 10.1016/j.sse.2009.12.004.

Licinus Benea received hid PhD in Micro and nanoelectronics from the University of Grenoble Alpes, France, in 2019. His research is mainly focused on the electrical characterization and simulation of SOI devices for various applications. Since 2020, he is a research engineer in CEA Grenoble developing the FD-SOI technology towards cybersecurity applications.

Melania Popescu received her PhD in Biological Sciences in 2018, at the Faculty of Biology-University of Bucharest, Romania. Her doctoral theme was on development of biochips for high-throughput detection and analysis of biomolecules. Its accomplishment required to combine knowledge in surface chemistry, materials characterization, genetics, bioinformatics, image and data analysis.

Maryline Bawedin received the Ph.D. degree from the Catholic University of Louvain, Louvain, Belgium, and the National Polytechnic Institute of Grenoble, Grenoble, France, in 2007. She is currently an Associate Professor with Grenoble INP Minatec, Grenoble.

Monica Simion completed her doctorate at the Polytechnic University of Bucharest in 2011 and also since 1994 she has carried out her research activity in the National Institute for Research and Development for Microtechnology. The object of his research was the development of nanostructured materials and biosensors with applications in genetic diagnosis. She is currently working on developing devices for early diagnosis of fetal malformations.

Irina Ionica received the PhD in Micro and nano electronics from the National Polytechnic Institute in Grenoble, France, in 2005. Since 2006, she is associate professor at Grenoble Institute of Technology and develops her research activities at IMEP-LAHC laboratory, Minatec. Her current research interests include electrical characterization of silicon-on-insulator (SOI) substrates, sensing with ISFET-like structures, second harmonic generation for dielectric-semiconductor interfaces characterization, nano-characterization by scanning probe microscopy.